

Improving efficiency of wireless charging system in electric vehicle using a hybrid ultracapacitor-battery energy storage approach

Liew Hui Fang¹, Muhammad Izuan Fahmi Romli¹, Rosemizi Abd Rahim²,
Nurhakimah Mohd Mukhtar¹, Norhanisa Kimpol¹

¹Centre of Excellence for Renewable Energy (CERE), Faculty of Electrical Engineering and Technology,
Universiti Malaysia Perlis (UniMAP), Perlis, Malaysia

²Faculty of Electronic Engineering and Technology, Universiti Malaysia Perlis (UniMAP), Perlis, Malaysia

Article Info

Article history:

Received Feb 29, 2024

Revised May 11, 2024

Accepted Jun 20, 2024

Keywords:

Battery charges

Electric vehicles

Hybrid energy storage

Ultracapacitor (supercapacitor)

Wireless charging system

ABSTRACT

This research aims to enhance the efficiency of wireless charging systems in electric vehicles by integrating a hybrid ultracapacitor-battery energy storage solution. Traditional standalone battery-based energy storage systems in wireless charging often face sub-optimal charging efficiency, resulting in extended charging times and reduced energy transfer efficiency. To address this limitation, we propose a hybrid approach that combines the rapid charging capability of ultracapacitor (supercapacitor) with the long-term storage capacity of batteries. The optimal charging range is 0 cm to 2 cm, and the combined output voltage and current are 5 V to 12 V and 0.63 A, respectively. This hybrid energy storage system will significantly boost electric vehicles (EVs) charging efficiency. Our research involves experimental evaluation and data analysis to assess crucial parameters, including charging efficiency, energy transfer efficiency, and charging time. The experimental results are validated and compared against existing battery-only systems, shedding light on the advantages and limitations of the hybrid approach. This study contributes to the optimization of wireless charging systems, enhancing energy transfer efficiency, and promoting the broader adoption of wireless charging technology in electric vehicles.

This is an open access article under the [CC BY-SA](#) license.



Corresponding Author:

Liew Hui Fang

Centre of Excellence for Renewable Energy (CERE), Faculty of Electrical Engineering and Technology,
Universiti Malaysia Perlis (UniMAP)

02600 Arau, Perlis, Malaysia

Email: hfliew@unimap.edu.my

1. INTRODUCTION

With global warming and climate change concerns rising, the automobile industry is shifting towards electric vehicles (EVs) to reduce emissions. Stringent emission regulations aim to curb air pollution, fostering a greener environment. Major manufacturers like Toyota, Honda, Nissan, BMW, Mercedes-Benz, Tesla, and Audi are electrifying vehicles to achieve zero emissions [1]. Downsized internal combustion engines with turbocharging and supercharging are common in many EVs. Countries such as Germany, China, and Japan support EV development [2]. While plug-in charging is prevalent, wireless charging, used in EVs and low-power devices like smartphones, is gaining traction. Wireless power transfer (WPT) eliminates the need for wires between EVs and chargers, promoting cable-free power delivery.

A battery typically has high energy density but low power density, whereas an ultracapacitor possesses high power density but low energy density. Therefore, this paper proposes integrating multiple storage technologies to create a hybrid energy storage system (HESS), incorporating both batteries and ultracapacitors, aimed at enhancing the driving range of electric vehicles (EVs). To minimize the HESS size and improve the EV driving range, an optimization problem is formulated and solved using wireless charging technology, eliminating the need for physical cables. With wireless charging, users can simply place their device on a charging pad or surface, reducing the hassle of dealing with cords and connectors. Finally, the convenience of wireless charging makes it easier for users to charge their devices without the need to plug and unplug cables. This study defines the optimum EV configurations, with the best-selected configurations contributing to a reduction in electronic waste and environmental impact.

These WPT techniques enable the efficient transmission of electric power from one point to another through a vacuum or the atmosphere without the use of wires or other physical substances [3]. WPT technology utilizes inductive coupling to transmit power from a transmitter to a resistive load, as demonstrated in studies by Yadlapalli *et al.* [3] in 2022 and Deshmukh *et al.* [4] in 2022. With WPT techniques, power can be transmitted in three categories: short-range using inductive coupling coils, mid-range using resonant induction, or high range through electromagnetic wave power transfer. Therefore, wireless charging technology has a high likelihood of becoming a significant trend in the future.

However, the performance and battery lifespan of electric vehicles depend on a well-organized battery arrangement meeting various demands [5], [6], with efficiency and internal resistance being crucial. Battery replacements may lead to additional costs due to limited lifetimes. While a larger battery could address this, it would increase the vehicle's weight, potentially affecting performance [7], [8]. An alternative solution involves implementing a hybrid energy system, combining batteries with supercapacitors, offering high power and fast charging [9]. Supercapacitors can provide extra energy or power when the battery fails. The research aims to manage power and energy in a hybrid energy storage device [10], [11].

Ultracapacitor technology is increasingly popular for pulse power and backup applications, especially in electric vehicles (EVs). Combining batteries with supercapacitors in EVs improves performance and durability. However, since supercapacitors discharge quickly, they complement batteries, which have lower specific energy and smaller capacity. This hybrid system optimizes power delivery during acceleration, thus prolonging battery life [12], [13]. Despite being the standard for EVs, plug-in charging presents safety and convenience issues. Contact charging, especially with high-voltage batteries, can cause sparks, and adverse weather can damage cables, leading to short circuits [14]–[16]. Wireless charging also requires drivers to leave their vehicles and can be time-consuming depending on the charger's power level [17], [18].

In 2018, Gong *et al.* [19] explored a wireless charging method for EVs with smart control. This system includes features such as battery status tracking and real-time regulation of charging voltage and current, all displayed on a screen. The charging process involves multi-stage charging, utilizing both constant current and constant voltage (CC-CV) methods, achieved by switching between two compensation networks, namely bilateral L3C and L3C-C. Throughout the charging process, the battery's state information is collected by a battery management system using wireless communication, and the battery's state is assessed. Subsequently, the controller activates the power supply and adjusts the output power according to the charging parameters, which are determined based on the battery's state. This approach ensures that the battery information transmitted to the controller through Wi-Fi communication is both faster and more stable, allowing the charging process to be controlled by the controller, taking into account the battery information displayed on the LCD screen. As a result of this advanced control system, the charging time is reduced by 16% compared to traditional constant voltage charging. Specifically, the charging time for this system is 150 minutes, whereas traditional constant voltage charging takes 180 minutes. The WPT system achieves an impressive efficiency rate of about 92%.

In 2022, Prasanthi *et al.* [20] proposed a hybrid energy storage system (HESS) for electric vehicles. This system involves the parallel connection of both a battery and a supercapacitor, with each side connected to a bidirectional DC-DC converter. The setup included a battery-only single-source energy storage system for comparison with the supercapacitor and battery HESS, and the simulation was conducted using MATLAB. The system consisted of 12 lead-acid batteries connected in series with ratings of 144 V and 2.2 Ah, 5 ultracapacitors connected in series with ratings of 210 V and 30 F, and 5 HP 240 V DC motor. During the braking mode, the rate of increase in the state of charge (SOC) for the battery-only energy storage system is slower when compared to the battery-ultracapacitor hybrid energy storage system. Additionally, the battery-ultracapacitor hybrid energy storage system achieves the desired voltage rise and speed more quickly than the battery-only energy storage system, both in the motoring and braking modes. The bidirectional DC-DC converter operates in two modes: boost mode when supplying power to the DC motor and buck mode when capturing regenerative power from the DC motor during the braking mode.

In the studies [21], [22], another configuration of a battery-ultracapacitor HESS was explored, specifically, a modified semi-active HESS. This system features a Panasonic NCR 18650B battery pack with

ratings of 23 V to 28 V and 54 Ah and a Maxwell ultracapacitor module (BCAP0350) with ratings of 16 V and 100 F. In this battery-ultracapacitor HESS configuration, the ultracapacitor is connected to the bidirectional DC-DC converter, while the battery is directly connected to the load. When transient current events requiring supply are halted, the battery begins to charge the ultracapacitor, while still providing current to the load. Compared to the configuration reviewed in [23], [24], the suggested battery-ultracapacitor HESS is classified as a full-active HESS, as it features a bidirectional DC-DC converter on both sides of the ultracapacitor and battery. In the simulation results from MATLAB, the current supplied to the load by the battery remains unchanged both under normal operating conditions and during periods of high load demand, typically at 20 A. When the high load current demand reaches 100 A, the ultracapacitor's SOC starts to discharge to around 80%, and the load requires 80 A of current.

In accordance with the findings from an energy management algorithm was developed for an electrical hybrid vehicle [25]. In this system, the fuel cell serves as the primary energy source, while the ultracapacitor and battery act as the main energy storage systems. The fuel cell, as the primary source, generates the necessary energy for the EVs. During acceleration, any power deficit is supplemented, while excess power is absorbed during braking operations. The power from the three energy sources is accurately regulated by determining the converters' current using the energy management algorithm. A bidirectional DC-DC current converter is employed to convert the variable voltage into a constant voltage for the battery. The energy management system used in the hybrid vehicle is primarily focused on distributing the energy flow among the various sources of the electric vehicle.

In 2019, Rozman *et al.* [26] introduced a smart wireless charging system for electric vehicles, which employs location-based car charging with sensors placed under the vehicle's wheels to determine its position. To activate the transmitter coils in the charging pad, the vehicle must be parked within a marked parking area, allowing the sensors to detect the wheels. There are 16 sensors used in the parking area, arranged in a 4×4 matrix, with each set of four sensors determining the position of one of the vehicle's wheels. In addition to the sensors, there are 6 transmitter coils, each connected to a separate relay on the switching board. To determine the vehicle's charging position, it's necessary for at least two wheels to be detected by the sensors. The experimental results show that there can be a maximum misalignment of 50% between the transmitter coil and the receiver coil. The coverage between these two coils ranges from 100% to 25%. As the misalignment between these two coils increases, the efficiency of power transfer decreases. In this smart wireless charging system, it takes 2 seconds per coil to determine the most suitable coil for charging.

In 2022, Mohamed *et al.* [27] detailed the implementation of a fast charging feature using wireless charging technology, incorporating a 12 V, 1.3 Ah battery. High-frequency RF antennas served as both transmitters and receivers for wireless power transfer (WPT), aiming to minimize losses [28]-[32]. Operating at frequencies of 2.4 GHz and 5.8 GHz, these antennas enhanced power transfer efficiency. An advanced fast charging technique utilized a 3-step battery charger, initially rapidly charging the battery until a predetermined voltage, then regulating current flow, and finally charging optimally. This approach increased battery voltage from 35% to 65% in 30 minutes with a load and up to 90% without a load, showcasing reduced heat generation during fast charging [33]-[35]. The research's primary goal is to address power and energy management challenges in hybrid energy storage devices, emphasizing the advantages of supercapacitors in various applications, particularly in pulse power and backup sources. Combining batteries and supercapacitors preserves battery life cycle and enhances EV performance. The proposed hybrid energy storage system integrates three 18650 lithium-ion batteries (5 V, 2200 mAh) as primary energy storage and four 3.0 V ultracapacitors (40 F each) as secondary storage. Induction power transfer facilitates wireless charging, transferring power from a primary coil to a secondary coil [36], [37].

The study focuses on optimizing the system's design for maximum efficiency and reliability by selecting appropriate components such as boost converter and spiral as wireless coil, designing efficient CC-CV charging mode, and implementing robust control strategies [38], [39]. Furthermore, the research aims to evaluate the performance of the hybrid ultracapacitor-battery energy storage approach through comprehensive testing and analysis, assessing factors such as charging time, energy efficiency, system stability, and overall reliability to validate the effectiveness of the proposed design. In summary, section 1 introduces the concept of wireless charging systems for EVs and underscores the need to enhance their efficiency. Section 2 outlines the experimental setup and simulation methodology, as well as the criteria for selecting ultracapacitors and batteries, and describes how they are integrated into the wireless charging system. Section 3 provides a detailed analysis of the results and discussions, including the performance and efficiency of the system. Finally, the research concludes with a summary of findings and discusses the implications in the concluding section.

2. METHODOLOGY

The research proposes integrating batteries and ultracapacitors in a hybrid energy storage system (HESS) to ensure energy stability. The system's performance is evaluated by monitoring state of charge (SOC)

changes in both components. Initially, power is supplied from an AC source and adjusted to the desired voltage using a step-down transformer. Figure 1 illustrates the primary power supply from the AC source, stepped down by a transformer before reaching the primary coil. One side of the primary coil acts as a transmitter, delivering power to the receiver coil. The received AC power is converted to DC using an AC-DC converter, then regulated to a specific voltage (typically 5.0 V to 13.0 V) suitable for charging the HESS.

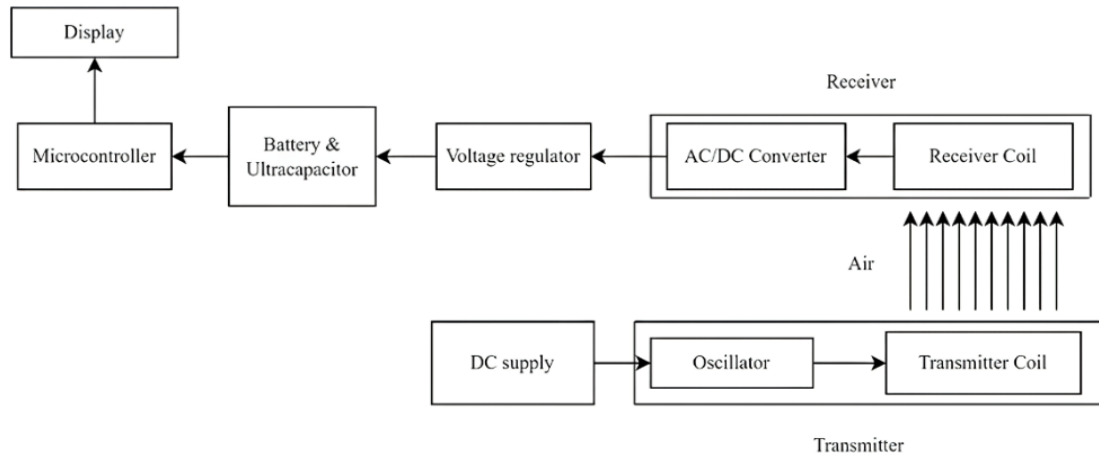


Figure 1. Wireless hybrid storage device charging station for HESS

2.1. Design of hybrid energy storage system circuit

Figure 2 illustrates the block diagram design of the recommended hybrid energy storage system, and the performance analysis of the energy storage system is conducted using Simulink, a MATLAB software. In this configuration, four ultracapacitors with a voltage rating of 3 V and a capacity of 40 F are connected in parallel to the energy source of the HESS. Additionally, a DC-DC converter is connected to and safeguards three 18650 lithium-ion batteries, each with a voltage rating of 5 V and a capacity of 2200 mAh, to effectively control the energy flow. The balance of power between the battery and the ultracapacitor is maintained by the DC-DC converter connected in series. This connection results in a combination of the battery and ultracapacitor with a total nominal voltage of 15 V and a capacity of 2200 mAh. Meanwhile, the ultracapacitors, connected in series, contribute to a total voltage of 12 V and a capacitance of 10 F. The charging circuit prioritizes monitoring the SOC for both the batteries and ultracapacitors.

2.2. Development of parameters for transmitter coil and receiver coil in WPT

The wireless charging system employs the concept of induction power transfer, where the transmitted energy relies on a primary coil in the transmitter and a secondary coil in the receiver. Calculating the inductance value of a coil is crucial for designing an effective WPT system, as (1). The inductance of both the primary and secondary coils can be calculated using (1) [2], [31].

$$L = \frac{\mu \pi N^2 R}{2} \quad (1)$$

In (1), L represents the coil's inductance, N stands for the number of turns in the coil, μ equals $\mu_0 \mu_r$, where μ_0 represents the absolute permeability with a value of 4×10^{-7} H/m, and μ_r is the relative permeability (equal to unity). From (2), mutual inductance is directly proportional to the number of turns in both the primary and secondary coils, as well as the radius of the secondary coil. This means that if the number of turns is increased, the mutual inductance will also increase. The mutual inductance of the two coils can be calculated using (2) [2], [32].

$$M = \frac{\mu \pi n_1 n_2 A}{l} \quad (2)$$

In (2), n_1 represent the number of turns in the primary coil, n_2 signify the number of turns in the secondary coil, A denote the cross-sectional area in square meters, and l indicate the coil length in meters. In the energy management system of wireless charging, an investigation into the optimal charging distance range

will be conducted, taking into account the distance between the transmitter coil and the receiver coil. During the coupling coefficient test, it's observed that the coefficient of coupling between the coils decreases as the air gap between the transmitter and receiver increases. The coil used in this context is a circular planar coil, chosen for its higher coupling coefficient and misalignment tolerance when compared to a square planar coil. Consequently, the coupling coefficient can be calculated using (3) [2].

$$K = \frac{M}{\sqrt{L_1 L_2}} \quad (3)$$

In (3), where the symbol K represents the coefficient of coupling, M stands for the mutual inductance of coils, L_1 denotes the inductance of the primary coil, and L_2 represents the inductance of the secondary coil. The design is divided into three parts: primary side design, secondary side design, and a monitoring system created using Proteus 8 software. The module used is a 9 V wireless charging module, consisting of a transmitter module and a receiver module. Each module comprises 10 turns of wire capable of supporting the 9 V wireless charging module. Increasing the number of turns in the coil results in higher inductance, as more turns generate a greater magnetic field. The inductance generated by 10 turns of coils is 7.85, as calculated using (1).

The input voltage required by the module is 12 V, and it can support a maximum input voltage of 13.5 V, making it compatible with most AC adapters that provide 12 V output voltage. The output power from the module is approximately 5.4 W, with an output voltage of 9 V and an output current of 0.6 A. Figure 3 illustrates the connection of the primary side of the transmitter coil in the wireless charging system.

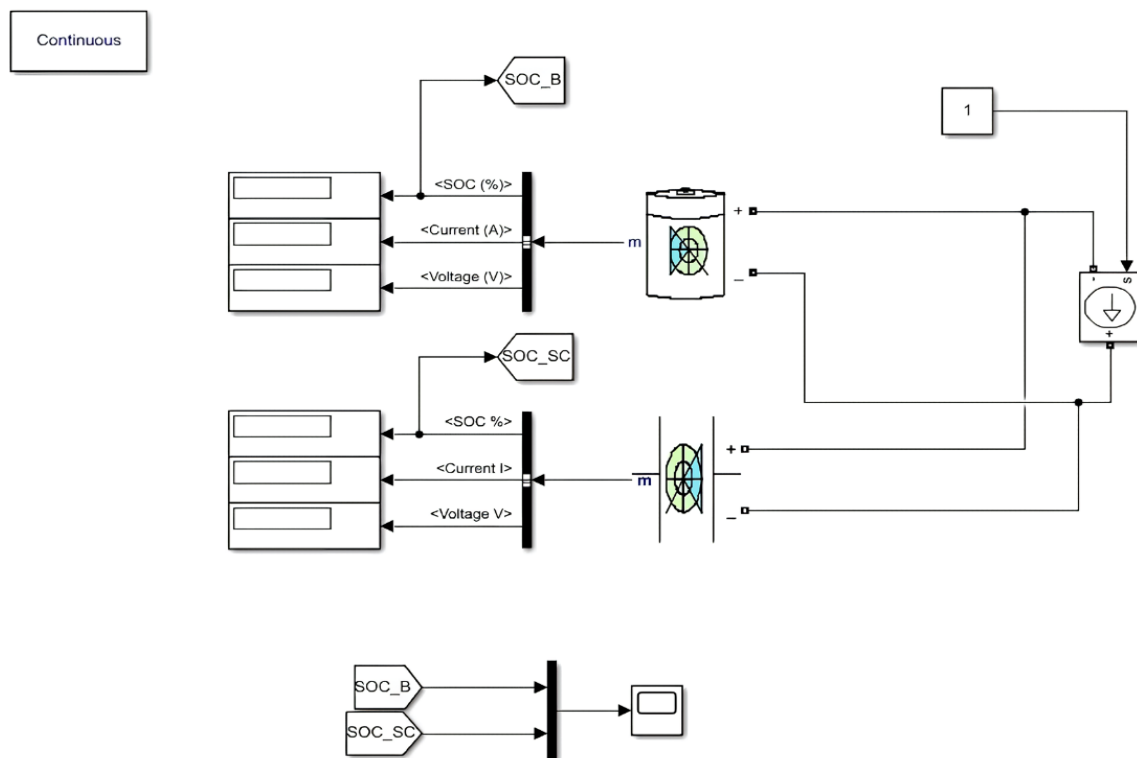


Figure 2. Hybrid storage system (ultracapacitor and battery) design

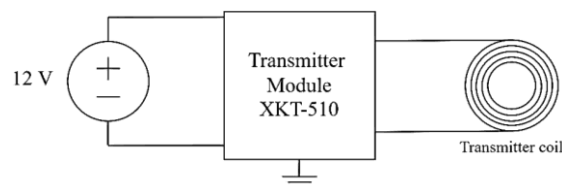


Figure 3. The primary side of transmitter coil circuit with a wireless charging system

2.3. Development of the secondary side of the receiver module in the wireless charging system

On the secondary side features a receiver module that pairs with the transmitter module. This receiver module includes a bridge rectifier and a filter capacitor to convert the received AC supply into DC and reduce ripple voltage. As the output DC voltage from the wireless charging module is insufficient at 9 V, a DC-DC boost converter XL6009 is employed to increase it to the desired 13 V for charging both the 11.1 V 18650 lithium-ion batteries and the 12 V, 10 F ultracapacitors in the HESS system. Figure 4 illustrates the proposed receiver coil circuit within the wireless charging system. The experiment involves assessing the output voltage both without and with the boost converter connected. The distance between the transmitter and receiver coils is adjustable (0 cm to 5 cm), and changes in the output voltage are examined. Tuning both coils to the resonant frequency enhances energy delivery efficiency and range through magnetic resonance coupling techniques.

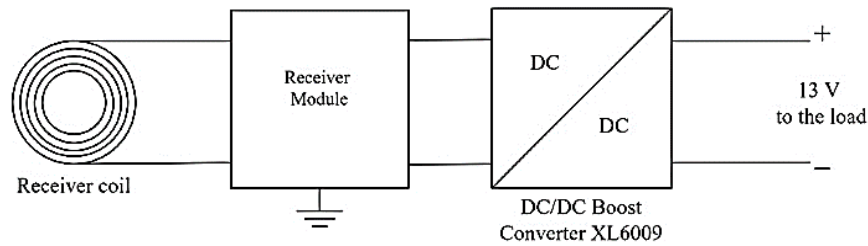


Figure 4. The secondary side of the receiver coil circuit with a wireless charging system

2.4. Development a battery charging circuit with a voltage regulator and current limiter

Figure 5 displays the simulation circuit used to control voltage and restrict current during the charging of lithium-ion batteries. This circuit was created using Proteus. Within the circuit, there are three sets of LM317T integrated chips configured as both current limiters and voltage regulators. The decision to maintain the voltage level at 5 V is based on the fact that the lithium-ion batteries are charged by individual single-cell lithium-ion battery charging modules (TP4056), each of which requires a supply voltage of 5 V. In the diagram, R7, R8, and R12 represent the TP4056 modules, which act as loads for charging the batteries.

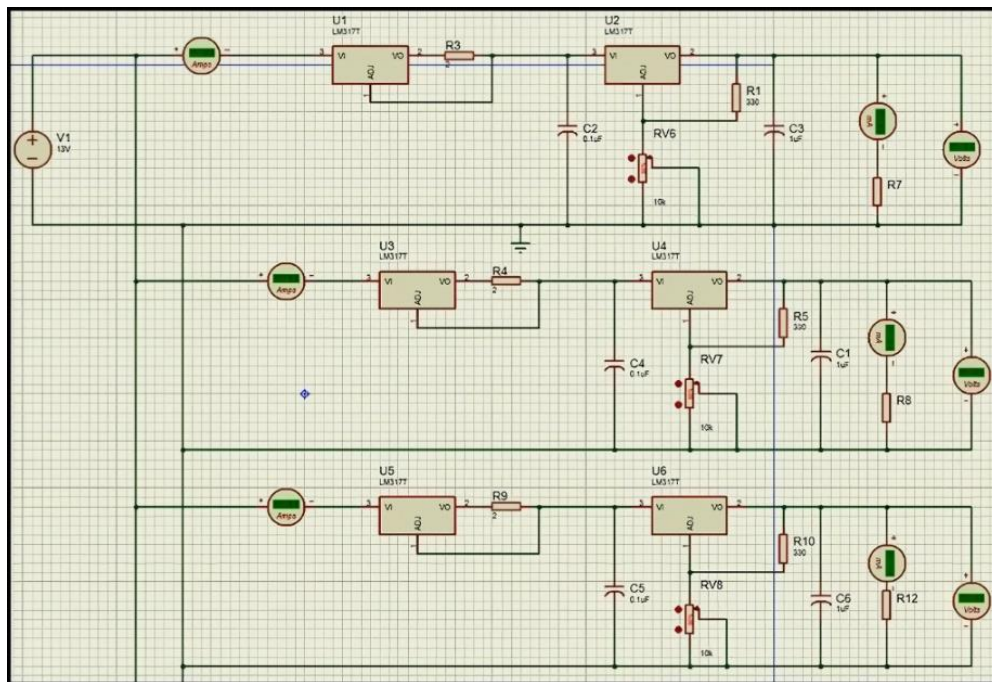


Figure 5. Battery charging circuit with voltage regulation and current limiter

Furthermore, the charging topology of the module is specific, using constant voltage and constant current charging, which is a necessary requirement during the battery charging process. The charging cell voltage from the module must adhere to a typical range of 2.4 V to 4.2 V. This voltage range is a common charging level for all lithium-ion batteries and must not be exceeded. If it does, the current flowing into the batteries gradually decreases or tapers until it approaches zero. During the initial stages of the charging process, the battery is charged in constant current mode as long as its voltage remains below 4.2 V. Once the battery voltage reaches approximately 4.2 V, the charging process transitions to constant voltage mode, where the charging voltage is maintained at 4.2 V until the charging current drops to a low value, typically less than 0.1 A. At this point, the charging process stops, and the battery is nearly fully charged. The CC-CV charging mode is an effective method for charging lithium batteries. When a lithium battery is nearly empty, it's important to ensure that the charging current is kept lower than the maximum current the battery can accept, as excessive current can lead to overheating or damage. During continuous charging, the battery voltage gradually increases. Once the battery voltage reaches the maximum charging voltage (in this case, 4.2 V), the charger maintains the charging voltage at this constant level and reduces the charging current. This helps to protect the battery and extend its lifespan. The purpose of the smoothing capacitor is to reduce the ripple in the pulsating DC voltage. In this case, the value of the smoothing capacitor is 0.1 μF . The calculation of the smoothing capacitor value is determined using (4) [27].

$$C = I \frac{\Delta t}{\Delta U} \quad (4)$$

In (4), the variables are defined as follows: C represents the capacitance of the desired smoothing capacitor, measured in μF . I represent the charge current of the circuit, measured in mA. Δt represents half the period of the circuit, measured in ms. ΔU represents the ripple voltage of the circuit, measured in V.

2.5. Design ultracapacitor charging circuit with voltageregulator and current limiter

The ultracapacitor serves as a secondary energy source and plays a critical role in providing high power when the motor requires it. The microcontroller takes on the responsibility of managing the charging and discharging processes of the ultracapacitor. This ultracapacitor can efficiently charge and discharge quickly, which contributes to its extended lifespan. Its rapid charging and discharging characteristics are well-suited to generating large amounts of energy in HEVs. Figure 6 illustrates the voltage regulation and current limiting circuit used for charging the ultracapacitors. As the four ultracapacitors are charged in separate circuits, this setup allows for the ultracapacitors to be charged in a balanced manner, ensuring that each receives an appropriate charge. The total voltage of the ultracapacitors during the experimental charging process is monitored.

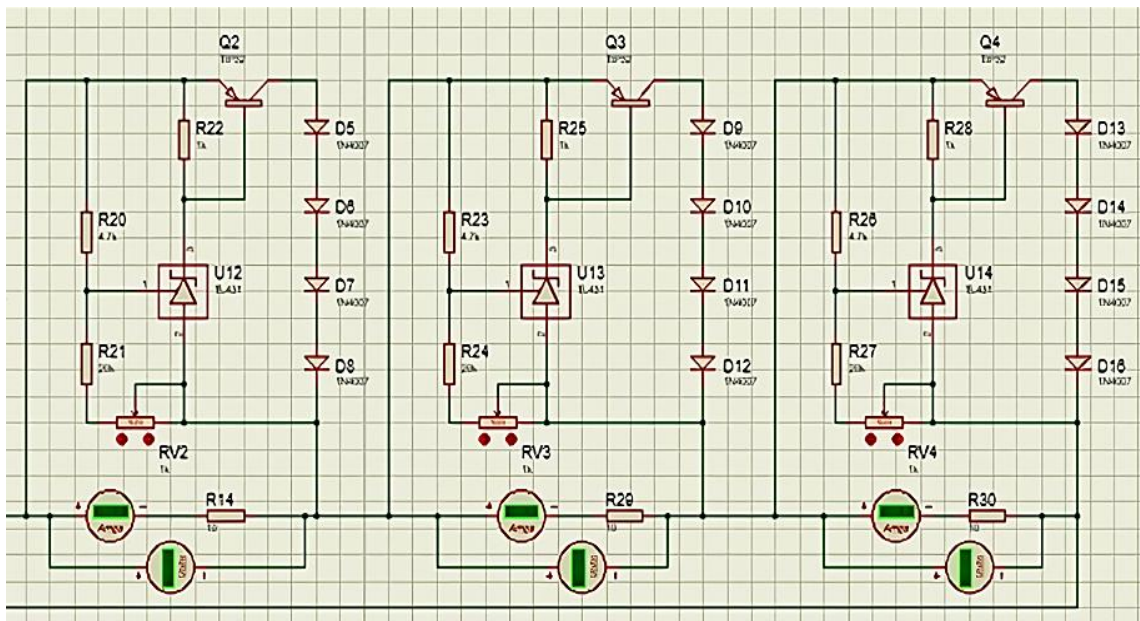


Figure 6. Ultracapacitor charging circuit with voltage regulator and current limiter

2.6. Design data display in charging monitor LCD

In addition to its role in this experiment, the monitoring system includes an LCD screen that displays essential information, such as the fully charged voltage and the SOC of the energy storage. Figure 7 and Figure 8 illustrates the experimental setup of the battery-ultracapacitor HESS, incorporating a wireless charging topology. The power supply and electronic load are regulated to simulate charging and discharging currents, respectively. The performance analysis of the HESS in HEVs involves the utilization of two different energy sources: the battery and the ultracapacitor. Specifically, a lithium-ion battery and a permanent magnet synchronous motor are employed in this analysis.

The microcontroller is responsible for managing the charging or discharging condition of the ultracapacitor, depending on the SOC of the battery. The specifications of the ultracapacitor and battery are provided in Table 1. The HESS is simulated under a fixed load with a time duration of approximately 300 seconds. The research objective focuses on the analysis of SOC performance in ultracapacitors and battery energy storage systems. It involves an examination of the charging and discharging processes of these storage systems and aims to determine the optimal charging distance range for a wireless system.

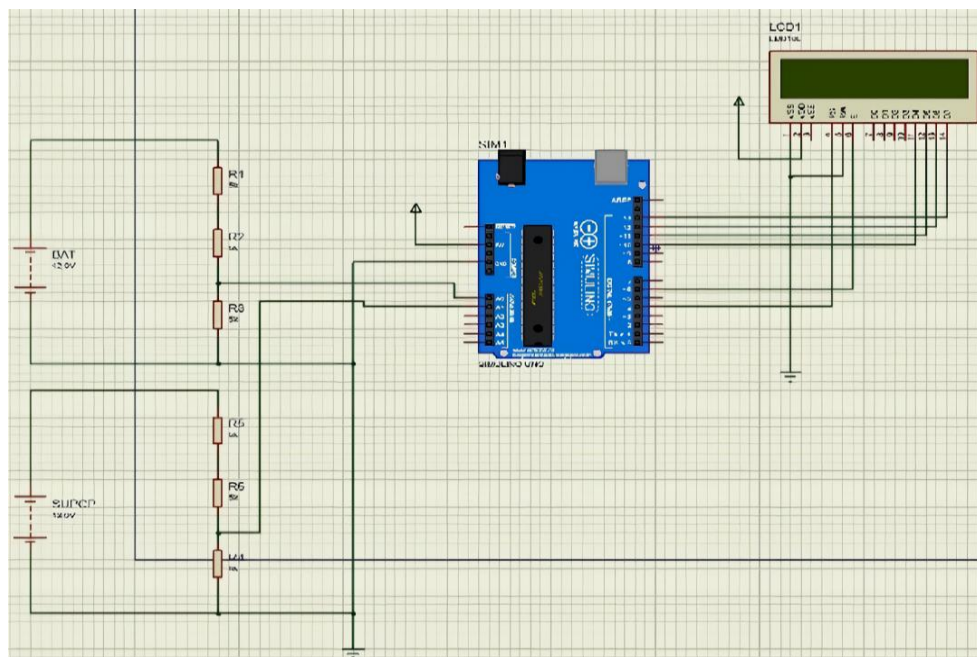


Figure 7. Ultracapacitor and battery charging circuit with Arduino UNO and LCD monitoring system

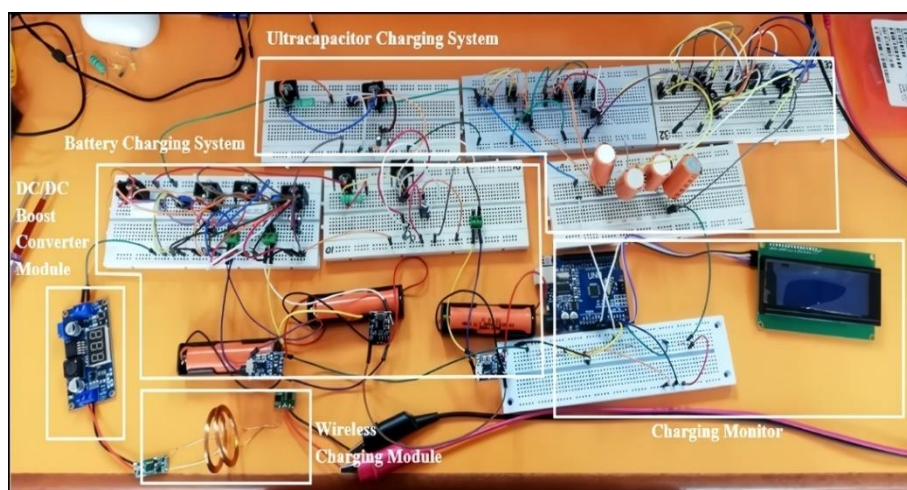


Figure 8. Experiment setup a wireless charging circuit and hybrid energy storage with a charging monitor

Table 1. Specifications parameters of ultracapacitor and lithium-ion battery

Lithium-ion battery		Ultracapacitor	
Nominal voltage	15 V	Rated capacitance/voltage rating	10 F/ 3 V
Rated capacity	2 Ah	ESR	0.075 Ω
Initial state-of-charge	100 % (discharging) and 0 % (charging)	Rated voltage	12 V
Cut off voltage	8.325 V	Number of series capacitors	4
Fully charged voltage	12.9203 V	Number of parallel capacitors	1
Nominal discharge current	0.8696 A	Initial voltage	12 V (discharging) and 0.08 V (charging)
Capacity at nominal voltage	1.8087 Ah	Operating temperature	25°C

3. RESULTS AND DISCUSSION

The simulation of the proposed passive hybrid energy storage system design is conducted using MATLAB software. In the simulation, lithium-ion batteries with a combined voltage of 15 V and a capacity of 2200 mAh are employed. These batteries are configured in series using three individual 5 V lithium-ion batteries. The charging and discharging of the batteries are carried out using a constant current technique set at 0.5 A. In a typical constant current mode battery charging system, the batteries are charged or discharged at a constant current until the desired voltage is attained.

3.1. Simulation result of lithium-ion battery analysis in charging and discharging condition

In Figure 9, the charging process and its effect on the SOC and voltage over time are presented. Figure 9(a) illustrates the increase in SOC of the lithium-ion battery from 0% to 100% in approximately 14,419.88 seconds, which is roughly 4 hours. Figure 9(b) shows the rise in voltage over time during the charging process. The battery's initial voltage increases from 9.56 V to 13.44 V in the same 14,419.88 seconds or about 4 hours. The fully charged voltage of the lithium-ion battery used is 12.92 V. During this time, the battery voltage experiences a rapid increase from 13.44 V to 24.13 V until it reaches a steady state after 14,419.88 seconds. Throughout this period, the SOC of the battery is approximately within the range of 90% to 100%, indicating that the battery is nearly fully charged. At this stage, the charge level in the lithium-ion battery is close to its maximum or saturation point. It's important to note that continuously charging the battery beyond this point could potentially lead to damage.

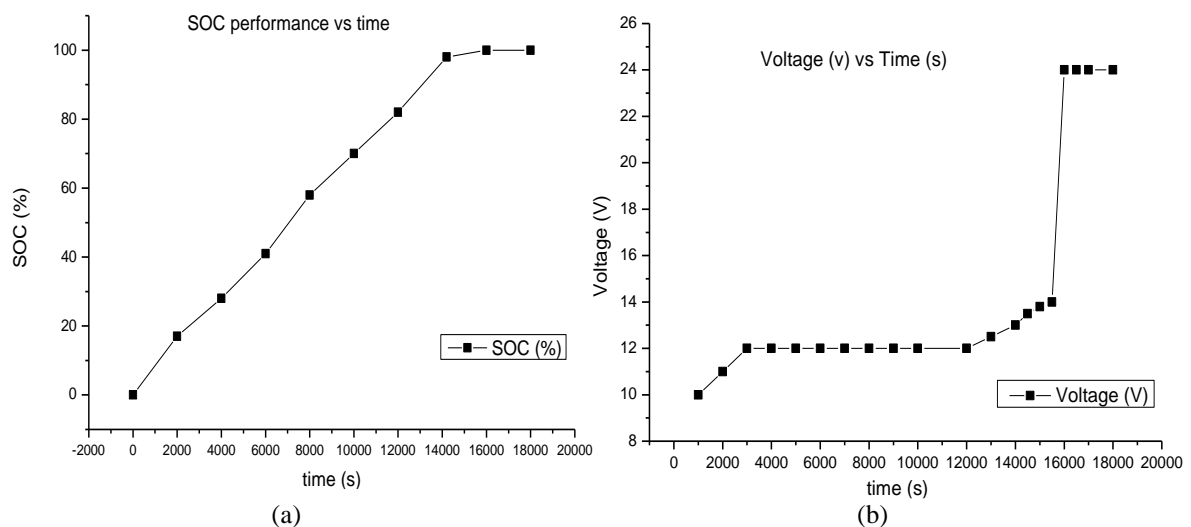


Figure 9. Lithium-ion battery against time on SOC changes performance during the charging process:
(a) SOC performance and (b) voltage increasing

Therefore, Figure 10 displays the changes in SOC and voltage during the discharging process. In Figure 10(a), it's shown that the SOC decreases from 100% to 0% in approximately 14,419.88 seconds, which also takes about 4 hours to complete the discharge. Figure 10(b) depicts the voltage drop over time during the discharging process. The voltage of the battery decreases from 12.91 V to 8.275 V in 14,419.88 seconds or about 4 hours. There is a sudden voltage drop from 8.275 V to 0 V when the voltage drops below 8.375 V. This drop occurs because the cut-off voltage for the lithium-ion battery has been set to 8.375 V. This value is

obtained from the simulation block parameters of the battery designed in Simulink. Therefore, the simulation cut-off voltage closely matches the cut-off voltage specified in the block parameters of the battery. Based on the simulation of the lithium-ion battery's performance, both the charging and discharging times are approximately 4 hours when a constant current of 0.5 A is maintained. However, it's important to note that without the implementation of any protection device or safety measures during charging, the battery may experience overcharging and a subsequent loss of capacity.

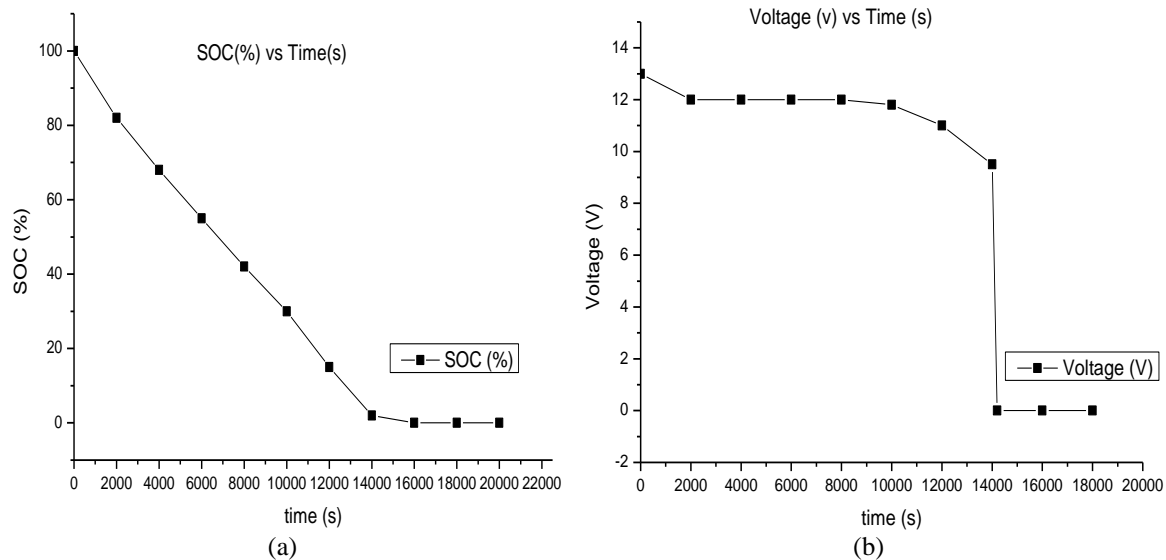


Figure 10. Lithium-ion battery against time on SOC changes performance during the discharging process
(a) SOC performance and (b) voltage decreasing

3.2. Ultracapacitor charging and discharging state analysis in the simulation result

This study examines the connection of ultracapacitors, where a series arrangement of four individual ultracapacitors with a voltage rating of 3 V and capacitance of 40 F results in a total series voltage of 12V and a combined capacitance of 10 F. The charging and discharging are conducted using a constant current mode set at 0.5 A. In Figure 11(a), it is demonstrated that ultracapacitor performance changes in terms of SOC and voltage increase during the charging process. The change in ultracapacitors' SOC performance increases from 0% to 100% in approximately 239.52 seconds, which is about 4 minutes. Ultracapacitors offer characteristics of high specific power and simple charging.

In Figure 11(b), the voltage rise of ultracapacitors overtime during the charging process is shown. The simulation results indicate that the voltage of the ultracapacitor increases from 0.08 V to 12.02 V in 239.52 seconds or about 4 minutes. When the ultracapacitors are nearly fully charged, the voltage reaches 12.02 V instead of 12 V. The tolerance and high energy density in ultracapacitors account for these characteristics.

Figure 12(a) displays the changes in SOC and voltage during the discharging process of ultracapacitors. The SOC of the ultracapacitor decreases from 99.89% to 0% in 239.52 seconds, which is about 4 minutes. Figure 12(b) shows the voltage drop of the ultracapacitor overtime during the discharging process. When the ultracapacitors are discharging, the voltage drops from 11.97 V to 2.39 V in 239.52 seconds or about 4 minutes. The voltage of the ultracapacitor starts to drop from 11.97 V instead of 12 V, primarily due to the self-discharge behavior of ultracapacitors.

The SOC of the ultracapacitors follows a similar trend, starting to drop from 99.89%. Ultracapacitors have low specific energy and a high self-discharge voltage. From the overall simulation results, the charging time and discharging time of the ultracapacitors are approximately 4 minutes each, with a constant current of 0.5 A for both processes. In addition, ultracapacitors offer several advantages, including an unlimited cycle life for charging and discharging in comparison to conventional batteries, low resistance, the capacity to handle high load currents within seconds, elimination of the need for end-of-charge termination, and a reputation for being safe to use.

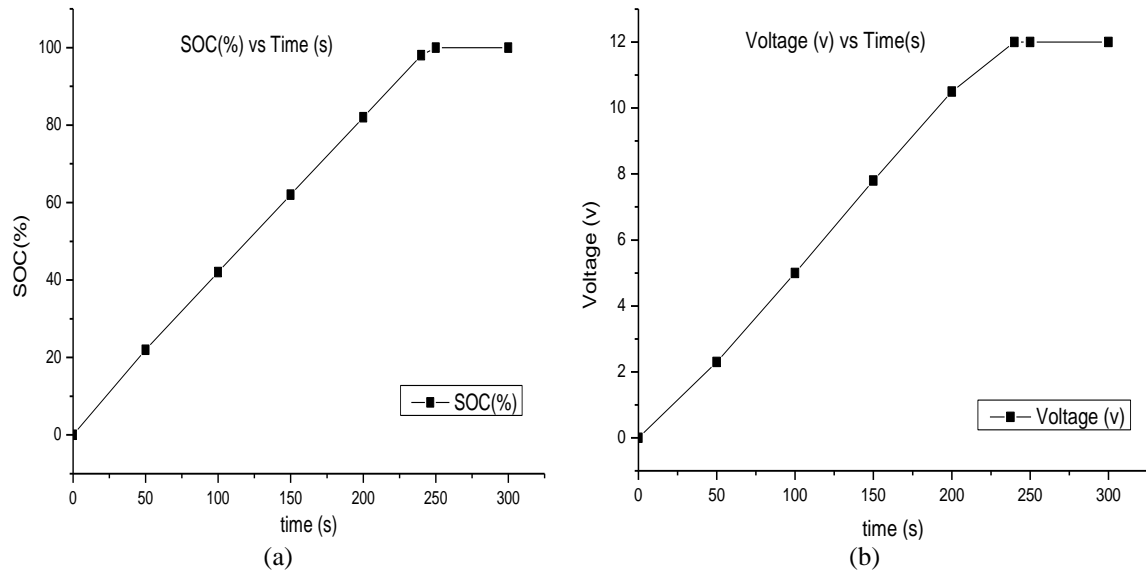


Figure 11. Ultracapacitors against time on SOC change performance during the charging process
(a) SOC performance and (b) voltage increasing

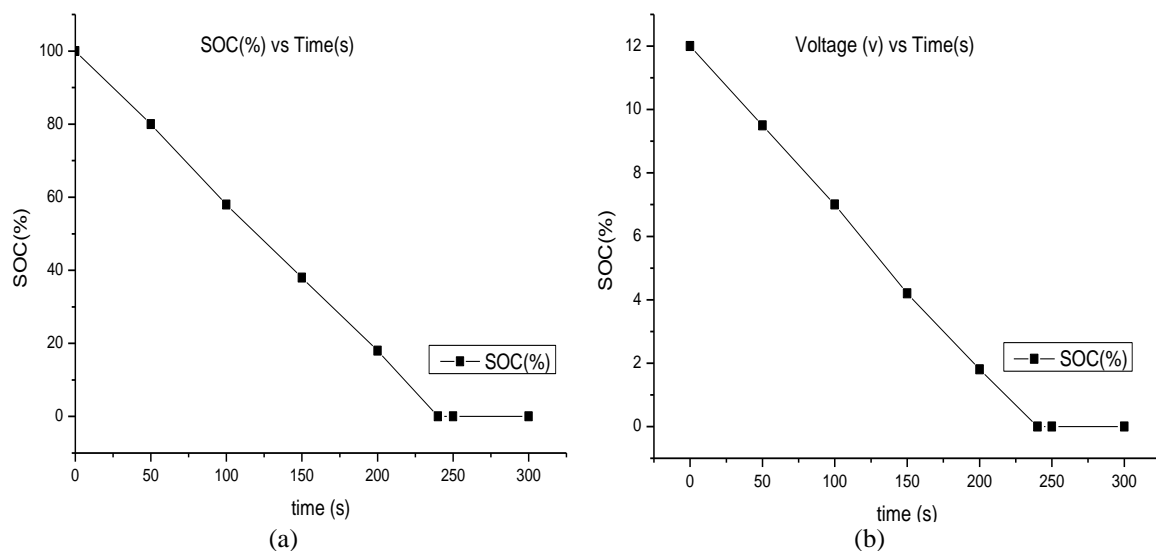


Figure 12. Ultracapacitors voltage against time on SOC changes performance during discharging process
(a) SOC performance and (b) voltage decreasing

3.3. Summary of comparison simulation result of lithium-ion battery and ultracapacitor in charging and discharging condition

Comparing the simulation results in Table 2 reveals that the charging time for the lithium-ion battery is longer than that of the ultracapacitor. The lithium-ion battery takes 240 minutes to reach a voltage of 13.44 V with 100% SOC, while the ultracapacitor achieves a voltage of 12.12 V with 100% SOC in just 4 minutes. This signifies the superior efficiency and time-saving charging capabilities of the ultracapacitor, achieving 100% SOC in only 4 minutes, which is 98% faster than the lithium-ion battery. The difference in charging performance can be attributed to the unique characteristics and sizing of the ultracapacitor, enabling it to have high power density and facilitate rapid bursts of power and faster charging. Both the ultracapacitor and lithium-ion battery are charged using the constant current technique at 0.5 A. Regarding discharging conditions, the ultracapacitor exhibits a rapid discharge, reaching 0% SOC within 4 minutes, and its voltage drops to 2.39 V. In contrast, the lithium-ion battery requires 240 minutes to reach 0% SOC, and its voltage drops to 8.275 V. The summary in Table 2 indicates that both charging and discharging times are the same, with a constant current of 0.5 A being applied.

Table 2. Summary comparison performance of lithium-ion battery and ultracapacitor during charging and discharging condition

Output performance parameter	Type of energy storage device	
	Battery	Ultracapacitor
Charging condition		
Specification using	18650 3.7, V Li-ion 2000 mAh	3 V, 40 F
SOC during charging	100%	100%
SOC charging time	240 min	4 min
Voltage maximum during charging	13.44 V	12.02 V
Time required during voltage maximum charging	240 min	4 min
Charging current	0.5 A	0.5 A
Discharging condition		
Specification using	18650 3.7 V, Li-ion 2000 mAh	3 V, 40 F
SOC during discharging	0%	0%
SOC discharging time	240 min	4 min
Voltage minimum during discharging	8.275 V	2.39 V
Time required during voltage minimum charging	240 min	4 min
Charging current	0.5 A	0.5A

3.4. Experimental result on investigating of optimum distance range on charging wireless charging system with or without boost converter

At the primary side, there is a transmitter module with an input supply of 12 V, and the secondary side features a receiver module. Table 3 provides the results of the output voltage obtained from the wireless charging module. Initially, the receiver module was tested without the boost converter. The boost converter is proposed to be used to maximize the highest output voltage and improve efficiency. The output voltage produced is approximately 9.06 V when the distance between the transmitter and receiver coils is varied from 0 cm to 1 cm.

However, when the distance is increased beyond 3 cm, the output voltage significantly decreases until it reaches 0 V. In the second testing scenario, the boost converter was integrated and connected to the receiver module, with the boost voltage set to 18 V. With the boost converter in place, when the separation distance increased from 0 cm to 1 cm, the output voltage was maintained around 18.07 V. However, when the separation distance increased to 1.5 cm or more, the output voltage decreased significantly until it reached 0 V. Consequently, the ideal charging distance falls within the range of 0 cm to 2 cm, where the lowest output voltage is measured at 15.03 V.

Table 3. Output of wireless charging module with and without boost converter

Distance (cm)	Input voltage, VIN (V)	Output voltage without boost converter, VOUT (V)	
		Output voltage without boost converter, VOUT (V)	Output voltage with boost converter, VOUT (V)
0.0	12	9.06	18.07
0.5	12	9.06	18.07
1.0	12	9.05	18.06
1.5	12	7.55	17.05
2.0	12	5.20	15.03
2.5	12	3.36	5.02
3.0	12	2.45	2.97
3.5	12	0	0
4.0	12	0	0
4.5	12	0	0
5.0	12	0	0

3.5. Comparison of simulation result and experimental result of energy management system in battery condition

On the secondary side, the battery charging circuit incorporates three pairs of LM317T integrated chips to power the TP4056 charging module. Additionally, a pair of LM317T integrated chips is utilized in the ultracapacitor charging circuit, arranged in a configuration that functions as both a voltage regulator and current limiter. Table 4 provides a comparison of the simulation and experimental results of the output voltage with a voltage regulator in the battery charging circuit. The voltage level is regulated to 5 V to supply the TP4056 module. According to the simulation results, the output voltage reaches 5.09 V when the input voltage is adjusted to 9 V. In the experimental setup, the output voltage is measured at 5.02 V when the input voltage is 9 V. Therefore, the output voltage is effectively regulated to 5 V when the input voltage is within the range of 9 V or higher, which is the target output for this system.

3.6. Comparison of simulation result and experimental result of energy management system in ultracapacitor condition

Table 5 provides the simulation and experimental results of the output voltage with a voltage regulator in the ultracapacitor charging circuit. In the simulation, the output voltage reaches 12 V when the input voltage is 18 V. During the experimental testing, with an input voltage of 18 V, the output voltage is measured at 12.03 V. This demonstrates that the output voltage remains regulated when the input voltage is 18 V or higher.

Table 4. Simulation and experimental result comparison output voltage from the regulator in battery charging circuit

Input voltage, V_{IN} (V)	Output voltage (simulation), V_{OUT} (V)	Output voltage (experiment), V_{OUT} (V)
1	0.00	0.01
2	0.06	0.16
3	0.68	1.21
4	1.61	1.86
5	2.46	3.09
6	3.30	3.99
7	4.12	4.81
8	4.87	5.01
9	5.09	5.02
10	5.09	5.02

Table 5. Simulation and experimental result comparison output voltage from voltage regulator in ultracapacitor charging circuit

Input voltage, V_{IN} (V)	Output voltage (simulation), V_{OUT} (V)	Output voltage (experiment), V_{OUT} (V)
2	0.04	0.21
4	1.51	2.11
6	3.23	4.02
8	4.98	6.24
10	6.74	7.88
12	8.50	10.07
14	10.24	11.76
16	11.98	12.01
2	0.04	0.21
18	12.00	12.03
20	12.00	12.03

4. CONCLUSION

In conclusion, the HESS used is combination of battery-ultracapacitor storage device in passive configuration. The wireless charging module operates between 0 cm to 2 cm and can boost output voltage to 18 V. Battery charging regulation begins at 18 V, with 5 V and 12 V output for batteries and ultracapacitors. Charging currents are limited to 0.63 A. Battery charging uses the TP4056 module and stops when the battery is nearly full. Ultracapacitor charging halts at 12 V. Charging times are 3 hours to 4 hours for batteries and 4 minutes to 5 minutes for ultracapacitors, showing the latter's faster energy storage. The CC-CV method is employed for battery charging. The system, driven by a microcontroller, can adjust voltage and current settings. Future research should focus on optimizing power flow management in the hybrid system, leveraging intelligent control algorithms like model predictive control, fuzzy logic, or neural networks for enhanced efficiency.

ACKNOWLEDGEMENTS

The author would also like to acknowledge Faculty of Electrical Engineering & Technology, Universiti Malaysia Perlis (UniMAP) for providing access to the laboratory and equipment and Chong Kah Hou for completing research data collection.

REFERENCES




- [1] I. Mahmud, M. B. Medha, and M. Hasanuzzaman, "Global challenges of electric vehicle charging systems and its future prospects: A review," *Research in Transportation Business & Management*, vol. 49, p. 101011, Aug. 2023, doi: 10.1016/j.rtbm.2023.101011.
- [2] S. Niu, H. Xu, Z. Sun, Z. Y. Shao, and L. Jian, "The state-of-the-arts of wireless electric vehicle charging via magnetic resonance: principles, standards and core technologies," *Renewable and Sustainable Energy Reviews*, vol. 114, p. 109302, Oct. 2019, doi: 10.1016/j.rser.2019.109302.
- [3] R. T. Yadlapalli, A. Kotapati, R. Kandipati, and C. S. Koritala, "A review on energy efficient technologies for electric vehicle applications," *J Energy Storage*, vol. 50, p. 104212, Jun. 2022, doi: 10.1016/j.est.2022.104212.

- [4] S. Deshmukh (Gore) *et al.*, "Review on classification of resonant converters for electric vehicle application," *Energy Reports*, vol. 8, pp. 1091–1113, Nov. 2022, doi: 10.1016/j.egy.2021.12.013.
- [5] M. Shafiei and A. Ghasemi-Marzbali, "Electric vehicle fast charging station design by considering probabilistic model of renewable energy source and demand response," *Energy*, vol. 267, p. 126545, Mar. 2023, doi: 10.1016/j.energy.2022.126545.
- [6] G. Saldaña, J. I. San Martín, I. Zamora, F. J. Asensio, and O. Oñederra, "Analysis of the Current Electric Battery Models for Electric Vehicle Simulation," *Energies (Basel)*, vol. 12, no. 14, p. 2750, Jul. 2019, doi: 10.3390/en12142750.
- [7] S. K. Rathor and D. Saxena, "Energy management system for smart grid: An overview and key issues," *International Journal of Energy Research*, vol. 44, no. 6, pp. 4067–4109, May 2020, doi: 10.1002/er.4883.
- [8] J. Deng, C. Bae, A. Denlinger, and T. Miller, "Electric Vehicles Batteries: Requirements and Challenges," *Joule*, vol. 4, no. 3, pp. 511–515, Mar. 2020, doi: 10.1016/j.joule.2020.01.013.
- [9] X. Li *et al.*, "Electric vehicle behavior modeling and applications in vehicle-grid integration: An overview," *Energy*, vol. 268, p. 126647, Apr. 2023, doi: 10.1016/j.energy.2023.126647.
- [10] B. Yang *et al.*, "Applications of battery/supercapacitor hybrid energy storage systems for electric vehicles using perturbation observer based robust control," *Journal of Power Sources*, vol. 448, p. 227444, Feb. 2020, doi: 10.1016/j.jpowsour.2019.227444.
- [11] N. M. Jamadar and H. T. Jadhav, "Effectiveness of supercapacitor during braking operation of electric vehicle," *Materials Today: Proceedings*, vol. 56, pp. 314–319, 2022, doi: 10.1016/j.matpr.2022.01.168.
- [12] K. V. Singh, H. O. Bansal, and D. Singh, "A comprehensive review on hybrid electric vehicles: architectures and components," *Journal of Modern Transportation*, vol. 27, no. 2, pp. 77–107, Jun. 2019, doi: 10.1007/s40534-019-0184-3.
- [13] N. Vukajlović, D. Miličević, B. Dumnić, and B. Popadić, "Comparative analysis of the supercapacitor influence on lithium battery cycle life in electric vehicle energy storage," *Journal of Energy Storage*, vol. 31, p. 101603, Oct. 2020, doi: 10.1016/j.est.2020.101603.
- [14] M. Brenna, F. Foia deli, C. Leone, and M. Longo, "Electric Vehicles Charging Technology Review and Optimal Size Estimation," *Journal of Electrical Engineering & Technology*, vol. 15, no. 6, pp. 2539–2552, Nov. 2020, doi: 10.1007/s42835-020-00547-x.
- [15] H. Yang, "A comprehensive study of supercapacitor Peukert constant dependence on voltage," *Journal of Energy Storage*, vol. 27, p. 101004, Feb. 2020, doi: 10.1016/j.est.2019.101004.
- [16] A. U. Rahman, I. Ahmad, and A. S. Malik, "Variable structure-based control of fuel cell-supercapacitor-battery based hybrid electric vehicle," *Journal of Energy Storage*, vol. 29, p. 101365, Jun. 2020, doi: 10.1016/j.est.2020.101365.
- [17] T. Zhu, R. G. A. Wills, R. Lot, X. Kong, and X. Yan, "Optimal sizing and sensitivity analysis of a battery-supercapacitor energy storage system for electric vehicles," *Energy*, vol. 221, p. 119851, Apr. 2021, doi: 10.1016/j.energy.2021.119851.
- [18] Z. Fu, Z. Li, P. Si, and F. Tao, "A hierarchical energy management strategy for fuel cell/battery/supercapacitor hybrid electric vehicles," *International Journal of Hydrogen Energy*, vol. 44, no. 39, pp. 22146–22159, Aug. 2019, doi: 10.1016/j.ijhydene.2019.06.158.
- [19] L. Gong, C. Xiao, B. Cao, and Y. Zhou, "Adaptive Smart Control Method for Electric Vehicle Wireless Charging System," *Energies (Basel)*, vol. 11, no. 10, p. 2685, Oct. 2018, doi: 10.3390/en11102685.
- [20] A. Prasanthi, H. Shareef, R. Errouissi, M. Asna, and A. Mohamed, "Hybridization of battery and ultracapacitor for electric vehicle application with dynamic energy management and non-linear state feedback controller," *Energy Conversion and Management: X*, vol. 15, p. 100266, Aug. 2022, doi: 10.1016/j.ecmx.2022.100266.
- [21] I. M. Abdelqawee, A. W. Emam, M. S. ElBages, and M. A. Ebrahim, "An improved energy management strategy for fuel cell/battery/supercapacitor system using a novel hybrid jellyfish/particle swarm/BAT optimizers," *Journal of Energy Storage*, vol. 57, p. 106276, Jan. 2023, doi: 10.1016/j.est.2022.106276.
- [22] H. Peng, J. Wang, W. Shen, D. Shi, and Y. Huang, "Compound control for energy management of the hybrid ultracapacitor-battery electric drive systems," *Energy*, vol. 175, pp. 309–319, May 2019, doi: 10.1016/j.energy.2019.03.088.
- [23] M. J. Lencwe, S. P. D. Chowdhury, and T. O. Olwal, "Hybrid energy storage system topology approaches for use in transport vehicles: A review," *Energy Science & Engineering*, vol. 10, no. 4, pp. 1449–1477, Apr. 2022, doi: 10.1002/ese3.1068.
- [24] E. M. Asensio, G. A. Magallán, C. H. De Angelo, and F. M. Serra, "Energy Management on Battery/Ultracapacitor Hybrid Energy Storage System based on Adjustable Bandwidth Filter and Sliding-mode Control," *Journal of Energy Storage*, vol. 30, p. 101569, Aug. 2020, doi: 10.1016/j.est.2020.101569.
- [25] H. Marzougui, M. Amari, A. Kadri, F. Bacha, and J. Ghouili, "Energy management of fuel cell/battery/ultracapacitor in electrical hybrid vehicle," *International Journal of Hydrogen Energy*, vol. 42, no. 13, pp. 8857–8869, Mar. 2017, doi: 10.1016/j.ijhydene.2016.09.190.
- [26] M. Rozman *et al.*, "Smart Wireless Power Transmission System for Autonomous EV Charging," *IEEE Access*, vol. 7, pp. 112240–112248, 2019, doi: 10.1109/ACCESS.2019.2912931.
- [27] N. Mohamed *et al.*, "A new wireless charging system for electric vehicles using two receiver coils," *Ain Shams Engineering Journal*, vol. 13, no. 2, p. 101569, Mar. 2022, doi: 10.1016/j.asej.2021.08.012.
- [28] J. Sun *et al.*, "A novel charging and active balancing system based on wireless power transfer for Lithium-ion battery pack," *Journal of Energy Storage*, vol. 55, p. 105741, Nov. 2022, doi: 10.1016/j.est.2022.105741.
- [29] N. Ali, Z. Liu, H. Armghan, and A. Armghan, "Double integral sliding mode controller for wirelessly charging of fuel cell-battery-super capacitor based hybrid electric vehicle," *Journal of Energy Storage*, vol. 51, p. 104288, Jul. 2022, doi: 10.1016/j.est.2022.104288.
- [30] R. Ye, X. Huang, Z. Chen, and Z. Ji, "A hybrid charging management strategy for solving the under-voltage problem caused by large-scale EV fast charging," *Sustainable Energy, Grids and Networks*, vol. 27, p. 100508, Sep. 2021, doi: 10.1016/j.segan.2021.100508.
- [31] L. Soares and H. Wang, "A study on renewed perspectives of electrified road for wireless power transfer of electric vehicles," *Renewable and Sustainable Energy Reviews*, vol. 158, p. 112110, Apr. 2022, doi: 10.1016/j.rser.2022.112110.
- [32] L. Sun, D. Ma, and H. Tang, "A review of recent trends in wireless power transfer technology and its applications in electric vehicle wireless charging," *Renewable and Sustainable Energy Reviews*, vol. 91, pp. 490–503, Aug. 2018, doi: 10.1016/j.rser.2018.04.016.
- [33] Y. Tian, W. Guan, G. Li, K. Mehran, J. Tian, and L. Xiang, "A review on foreign object detection for magnetic coupling-based electric vehicle wireless charging," *Green Energy and Intelligent Transportation*, vol. 1, no. 2, p. 100007, Sep. 2022, doi: 10.1016/j.geits.2022.100007.
- [34] S. Hemavathi and A. Shinisha, "A study on trends and developments in electric vehicle charging technologies," *Journal of Energy Storage*, vol. 52, p. 105013, Aug. 2022, doi: 10.1016/j.est.2022.105013.
- [35] Y. Zhang, Z. Huang, H. Wang, C. Liu, and X. Mao, "Achieving misalignment tolerance with hybrid topologies in electric vehicle wireless charging systems," *Energy Reports*, vol. 9, pp. 259–265, Sep. 2023, doi: 10.1016/j.egy.2023.04.278.
- [36] A. K. Podder, O. Chakraborty, S. Islam, N. Manoj Kumar, and H. H. Alhelou, "Control Strategies of Different Hybrid Energy Storage Systems for Electric Vehicles Applications," *IEEE Access*, vol. 9, pp. 51865–51895, 2021, doi: 10.1109/ACCESS.2021.3069593.
- [37] N.-D. Nguyen, C. Yoon, and Y. Il Lee, "A Standalone Energy Management System of Battery/Supercapacitor Hybrid Energy Storage System for Electric Vehicles Using Model Predictive Control," *IEEE Transactions on Industrial Electronics*, vol. 70, no. 5, pp. 5104–5114, May 2023, doi: 10.1109/TIE.2022.3186369.




- [38] S. M. Lukic, S. G. Wirasingha, F. Rodriguez, J. Cao, and A. Emadi, "Power Management of an Ultracapacitor/Battery Hybrid Energy Storage System in an HEV," in *2006 IEEE Vehicle Power and Propulsion Conference*, IEEE, Sep. 2006, pp. 1–6. doi: 10.1109/VPPC.2006.364357.
- [39] M. Ortuzar, J. Moreno, and J. Dixon, "Ultracapacitor-Based Auxiliary Energy System for an Electric Vehicle: Implementation and Evaluation," *IEEE Transactions on Industrial Electronics*, vol. 54, no. 4, pp. 2147–2156, Aug. 2007, doi: 10.1109/TIE.2007.894713.

BIOGRAPHIES OF AUTHORS






Liew Hui Fang    currently is a senior lecturer at Faculty of Electrical Engineering Technology from Universiti Malaysia Perlis. In 2012, she holds her degree in Electrical Systems Engineering at University Malaysia Perlis (UniMAP), Malaysia; in 2015, M.Sc. degree in Microelectronics Engineering from University Malaysia Perlis (UniMAP) and in 2018 she received the Ph.D. degree in Electrical Systems Engineering at University Malaysia Perlis (UniMAP). Her research interest includes the analysis and development of new sources of energy harvesting system and techniques, renewable energy, power energy, microwave communication, and RF MEMS. She can be contacted at email: hfliew@unimap.edu.my.






Muhammad Izuan Fahmi Romli    obtained his Ph.D. degree and master of science from University of Nottingham Malaysia Campus. In 2010, he received the bachelor of electrical engineering technology from Universiti Kuala Lumpur. Being active as an associate professor in the University Malaysia Perlis, his current interest lies on renewable energy, supercapacitor, optimization, and energy storage for electric vehicle. He can be contacted at email: izfahmi@gmail.com.






Rosemizi Abd Rahim    was born in Kedah, Malaysia in 1976. He received the B.Eng. degree in Electrical Engineering from Universiti Teknologi Mara, Malaysia, in 2000 and the M.Sc. degree in Electronic System Design Engineering from Universiti Sains Malaysia, in 2004. In 2013, he received the Ph.D. degree in Communication Engineering from Universiti Malaysia Perlis. From 2000 to 2004, he was a failure analysis engineer at a multinational electronic manufacturing company in Penang, Malaysia. His task was to resolve any failure that occur during the production process of electronic products. Then, since 2005, he has been moved to Universiti Malaysia Perlis as an academician. His research interest includes the analysis and development of new sources of energy harvesting system and techniques, antenna design and microwave engineering. Currently, he is a senior lecturer at Faculty of Electronics Engineering Technology at University Malaysia Perlis (UniMAP). He can be contacted at email: rosemizi@unimap.edu.my.



Nurhakimah Mohd Mukhtar    received her Ph.D. degree in Electrical Engineering in 2020, from the University of Sydney, Sydney, Australia. She is currently a senior lecturer and program chairperson of a Diploma in Electrical Engineering at the Faculty of Electrical Engineering and Technology, Universiti Malaysia Perlis, Malaysia. Her current research interests include power conversion for renewable energy sources, energy storage systems, and power electronics in power systems. She is presently a reviewer for journals such as IEEE Transactions on Industrial Electronics, and IEEE Journal of Emerging and Selected Topics in Power Electronics. She can be contacted at email: nurhakimah@unimap.edu.my.



Norhanisa Kimpol    obtained her master of engineering from Universiti Tun Hussein Onn Malaysia (UTHM). In 2023, she received the bachelor of electrical engineering (Hons) from Universiti Teknologi Mara (UiTM). Being active as vocational training officer in Universiti Malaysia Perlis, her current interest lies on renewable energy and power electronics. She can be contacted at email: norhanisa@unimap.edu.my.